Expedited Publication, Original Article

Propensity of aerosol and droplet creation during oculoplastic procedures: A risk assessment with high-speed imaging amidst COVID-19 pandemic

Roshmi Gupta, Khushboo Pandey[1], Rwituja Thomas, Saptarshi Basu[1], Bhujang Shetty[2], Rohit Shetty[3], Abhijit Sinha Roy[4]

Purpose: The study uses principles of liquid and gas mechanics to verify and quantify the generation of aerosols in oculoplastic procedures, namely surgery using a scalpel, electrosurgical device, and a mechanized drill. **Methods:** Surgical techniques were performed *ex vivo* using the electrosurgical device, scalpel, and mechanized drill on the muscle and bone of commercially available chicken. The liquid and gas dynamics were observed using a high-speed high-resolution Photron SA5 camera (0.125 to 8 ms temporal resolution, 0.016 to 0.054 mm/pixel spatial resolution) and stroboscopic lighting (Veritas 120 E LED Constellation). The analysis was performed using in-house algorithms and ImageJ software. **Results:** The use of a mechanized drill at 35000 rpm and a 3 mm fluted burr generated aerosol with particle size 50 to 550 microns with a spread of 1.8 m radius. Surgical smoke was generated by an electrosurgical device in both cutting and coagulation modes. Dispersion of the smoke could be controlled significantly by the use of suction, mean smoke spread ratio being 0.065 without suction and 0.002 with use of suction within 2 cm. **Conclusion:** The quantification of the aerosol generation will help surgeons take practical decisions in their surgical techniques in the pandemic era.

Key words: Aerosol, electrosurgical device, high-resolution high-speed imaging, surgical drill, surgical smoke

Videos Available on: www.ijo.in

Access this article online

Website: www.ijo.in

DOI: 10.4103/ijo.IJO_2859_20

Quick Response Code:

The COVID-19 pandemic has presented a healthcare burden to the healthcare community the world over. On October 17, 2020, 39,633,188 people have been infected worldwide, with 1,109,833 deaths.[1] The public health emergency is further compounded by the disruption to regular health care and the risk to health care personnel.[2]

The SARS-Co-V2 virus is transmitted chiefly through the respiratory tract, via droplet and air-borne particle spread.[3] With a large number of asymptomatic infections present in the population, any surgical procedure has the potential to infect health care workers.[4]

Ophthalmologists come in close contact with patients both during the outpatient examination and during surgery. There are indications that tears contain the viable virus in some patients.[5,6] In addition, oculoplastic procedures involve close contact with the nasal mucosa in the upper respiratory tract, which expresses entry-associated genes for SARS-CoV-2.[7] Oculoplastic surgery uses techniques of electrosurgery and high-speed automated saw and drill; these techniques are known to generate aerosols.[8]

Various specialty practice societies have issued guidelines for practice under these unprecedented circumstances. The guidelines combine previously published literature and expert opinions. The recommendations encompass use of suction during anesthesia, the use of electrosurgical devices, and the use of mechanized drill.[9-12]

The aerosols and droplets generated in the surgical procedures follow the physical principles of fluid (liquid and air) mechanics. We performed ex vivo experiments to demonstrate the generation of aerosols and droplets along with their spread distance in oculoplastic procedures and surgical techniques.

Methods

The study was performed in collaboration with the Department of Mechanical Engineering, Multi-phase Flow Studies Laboratory, Indian Institute of Science, Bangalore, India.

The muscle and bone of commercially available food-grade chicken (Gallus gallus domesticus) was carved and fixed onto a mannequin head used for surgical training, using cling film.

Orbit and Oculoplasty Services, Narayana Nethralaya, Bangalore, [1]Department of Mechanical Engineering, Indian Institute of Science, Bangalore, [2]Cataract Services, Narayana Nethralaya, Bangalore, [3]Cornea and Refractive Surgery Services, Narayana Nethralaya, Bangalore, [4]Imaging, Biomechanics and Mathematical Modelling Solutions lab, Narayana Nethralaya Foundation, Bangalore, India

Correspondence to: Dr. Roshmi Gupta, Ophthalmic Plastics, Orbital Disease and Ocular Oncology Service, Narayana Nethralaya, 121/C Chord Road, Rajajinagar 1st R Block, Bengaluru - 560 010, Karnataka, India. E-mail: roshmi_gupta@yahoo.com

Received: 02-Sep-2020 Revision: 07-Oct-2020
Accepted: 14-Jan-2021 Published: 17-Feb-2021

Cite this article as: Gupta R, Pandey K, Thomas R, Basu S, Shetty B, Shetty R, *et al*. Propensity of aerosol and droplet creation during oculoplastic procedures: A risk assessment with high-speed imaging amidst COVID-19 pandemic. Indian J Ophthalmol 2021;69:734-8.

The positioning of the experimental tissue over the upper and lower orbital rim simulated the location of the surgical field in oculoplastic surgery. A piece of flat bone of the chicken was placed in the socket of the mannequin, to simulate the deep position of the orbital wall. This is the area of interest in a decompression. The experiments were performed with the following protocols.

1. Surgical drill (Marathon Micromotor Model M4, South Korea, 35,000 rpm, 3 mm fluted burr drill bit) was used on the bone, with and without simultaneous irrigation.
2. The electrosurgical device (Ellman Surgitron FFPF EMC, New York, USA, in cutting and coagulation modes) was used on the tissue. This was used with and without a suction device (Goley Accu Hy Suc, India, suction 40–45 L/min, 3 Fr cannula at 1-2 cm distance).
3. Incisions were made on the tissue, with a number 15 Bard Parker surgical blade. The area was irrigated gently to simulate bleeding. A vacuum suction with a metal suction cannula of size 3 Fr was used simultaneously to aspirate the irrigation fluid.

To visualize the liquid motion and fluid dynamics during the experiments, the test section was volumetrically illuminated using the strobosopic lighting where the light source (Veritas 120 E LED Constellation) was kept perpendicuar to the camera [Fig. 1]. The technique of volumetric illumination provided a convenient way of transparent imaging objects (which in this case was saline). The liquid dynamics was acquired using a Photron SA5 camera coupled with a combination of macro-lens (Tokina 100 mm) and 36 mm extension tube. For Part 1 (drilling), the images were acquired at 8000 frames per second (1024 × 1024 pixel resolution and 0.125 ms temporal resolution). Zoomed-out (spatial resolution of 50 μm/pixel) and zoomed-in (spatial resolution 17 μm/pixel) imaging were done. For Part 2 of the experiments (surgical smoke), a green laser sheet (Laser MicroLine Generator from Schäfter + Kirchhoff with a sheet thickness of 120 μm) was employed to produce smoke scattering. The laser scattering was recorded using Photron SA5 camera coupled with a combination of macro-lens (Tokina 100 mm) and 36 mm extension tube at 125 frames per second (1024 × 1024 pixel resolution and 8 ms temporal resolution) and a spatial resolution of 54 μm/pixel.

Image processing

Image processing algorithms were performed using in-house ImageJ code on the acquired images. Using background substraction, the extraneous subjects such as hands of the surgeon, the drill and some of the mannequin areas were removed from the images. The resultant images were then binarized using Otsu thresholding.[13]

Part 1, Drilling: The technique of particle analysis was employed on binary images to evaluate the droplet shape descriptors such as area and bounding rectangle. For evaluating droplet trajectories, two-dimensional (2D) particle tracking technique with the Mosaic-suite plugin of ImageJ Software was utilized.[14] By varying the input parameters (kernel radii), multiple trajectories for several range of droplet dimensions were isolated. The results from the particle analysis were used to create a droplet size distribution map. Results of particle tracking were used to evaluate droplet ejection velocity and acceleration throughout their path-line.

The total distance traveled (x) by the droplets was calculated iteratively through computation using the following relations between the droplet of radius $r_{droplet}$ and velocity $u_{droplet}$:

$$\frac{dx}{dt} = u_{droplet}$$

$$\frac{du_{droplet}}{dt} = \frac{4.5\mu_{air}(u_{air} - u_{droplet})}{r^2_{droplet}\rho_{droplet}}$$

Where u_{air} represents the surrounding convection velocity (taken as 0.6 m/s),t is time, μ_{air} is the viscosity of the surrounding air, and $\rho_{droplet}$ is the liquid droplet density.

Part 2, Surgical smoke: The binary images were used to track the smoke area using particle analysis. The results from the particle analysis were then utilized to create a quantified time-history of the smoke spread. A spread parameter (s) was defined as the ratio of smoke area and the area of the region of interest (ROI) i.e., $s = A_{smoke} / A_{ROI}$

For all parts of the experiments, a dehumidifier in the range of 40–50% was used. The air speed was estimated as ~0.6 m/s (as per the certified inspection report of the operating theatres at the Narayana Nethralaya Eye Hospital). For analyses of spread of the droplets, the air flow was calculated as per the methods of our previous publications.[15,16] The properties of air at a temperature of 23°C were used in all the equations. Three sets of observations were obtained for each technique.

Results

Part 1 (Drilling): Droplet generation during medical drilling was experimentally investigated for droplet-size and velocity distribution. The analysis predicted maximum distance travelled by droplet during ejection.

The number of droplets generated increased with the simultaneous use of irrigation during drilling. For analyses, the results were calculated for the use of the drill on a wet field, without simultaneous irrigation. (Online supplementary material Video 1). Droplet generation from drilling was the outcome of imbalance between the centrifugal and liquid surface tension forces. Irrigation water near the drill rotated along with the burr. At high rotating speed (as in this case), the water layer was detached and elongated into ligaments. These ligaments underwent secondary atomization to form daughter droplets. The size distribution of the generated droplets is presented in Fig. 2. The predominant droplet size ranged from 50 μm to 550 μm. The droplet trajectories were dissimilar for smaller and larger droplets. The temporal variation of velocity values in vertical (V_Y) and horizontal (V_X) direction are presented for droplet size [Fig. 3a and b]. The smaller droplets traveled further in the y-direction, whereas bigger droplets had a decaying trajectory. The droplets' initial velocities were in the range of 0.5 m/s to 2.5 m/s. Hence, for displacement calculations [Fig. 4] these values were taken as the initial parameters along with the droplet diameter. The velocity and trajectory of the droplets predicted a spread radius of 1.8 m in our experiment.

Part 2 (Surgical Smoke) :

Qualitative observations: Surgical smoke was generated by the use of both monopolar (cutting mode) and

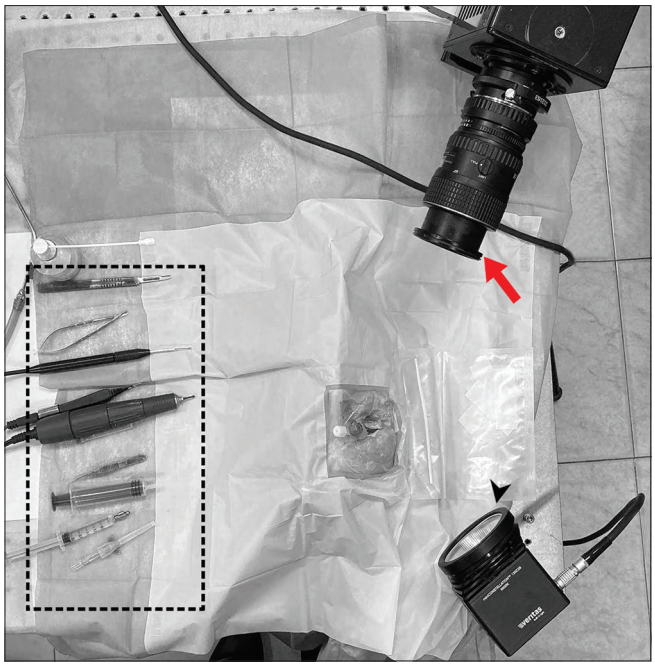

Figure 1: Experimental setup showing high speed camera, (red arrow), light source (black arrowhead), surgical instruments (black dotted box)

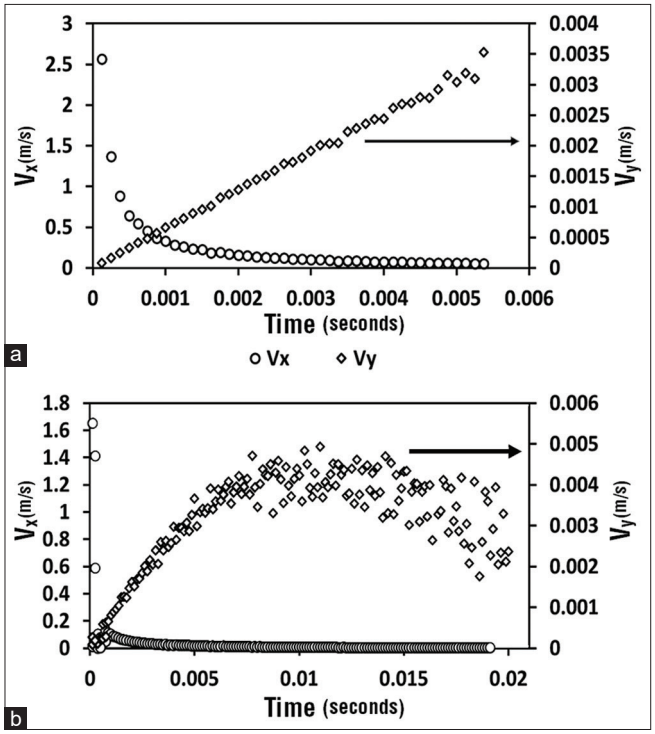

Figure 3: Temporal variation of the velocities in vertical (V_Y) and horizontal (V_X) for droplet size of (a) 150μm and (b) 400μm. The circle represents velocity along x-axis, the diamond represents velocity along y-axis

bipolar (coagulation mode) hand-pieces in the electrosurgical device. When the suction cannula was held close to the device (within 1–2 cm), the smoke could be suctioned into the cannula. If the distance was more than 2 cm, the smoke escaped and dispersed (Online supplementary material Video 2).

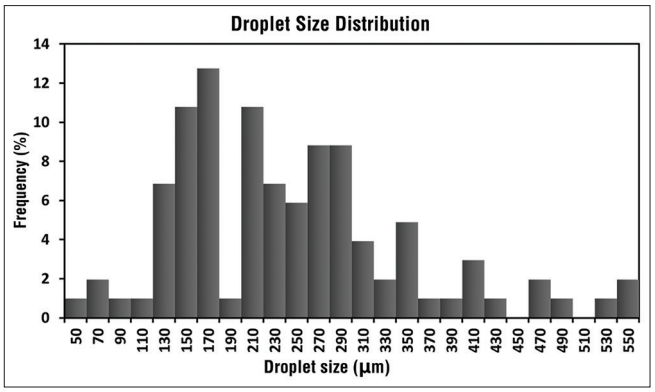

Figure 2: Graph showing droplet size distribution

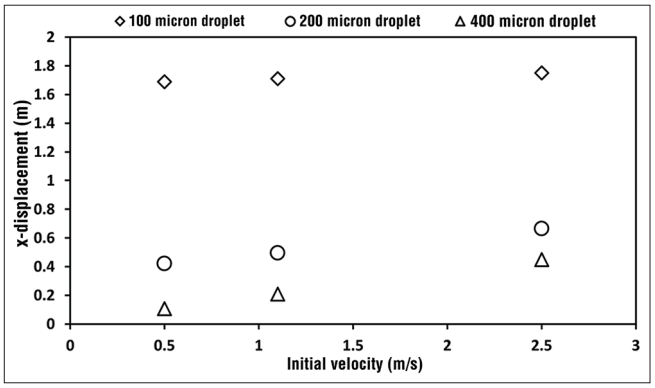

Figure 4: Variation of droplet displacement with variation in initial velocity for various droplet sizes. The diamond symbol represents a 100 μm droplet, the circle a 200 μm droplet, and triangle a 400 μm droplet

Quantitative Observations: In the current work, smoke generation and spreading dynamics during monopolar medical cautery were experimentally investigated with and without suction [Fig. 5]. Fig. 6 delineates the temporal variation of the smoke spread parameter for monopolar cautery with and without suction. The plot revealed reduction in parameter by an order with suction application with placement of the suction pipe at 2 cm. Furthermore, the parameter showed an oscillatory nature with time. Such oscillations were standard characteristics of a naturally buoyant plume i.e., motion of smoke due to its lower density as compared to its surrounding air. The maximum smoke spread ratio was 0.13 without use of suction, which changed to 0.005 with use of suction. The mean smoke spread ratio without suction 0.065 decreased to 0.002 with use of suction.

On the use of cold steel (scalpel and scissors) for incision and dissection- even with gentle irrigation and suction ongoing during the surgery, there was no droplet generation.

Discussion

Person to person transmission of the SARS-CoV2 virus occurs through close contact or by inhalation of aerosols into the respiratory tract.[17] Aerosols (aero-solutions) can be defined as a suspension of solid or liquid particles in a gas.[18] High speed surgical procedures are among the aerosol-generating procedures with documented higher risk of transmission of pathogens.[8] Surgical smoke (also called plume and cautery

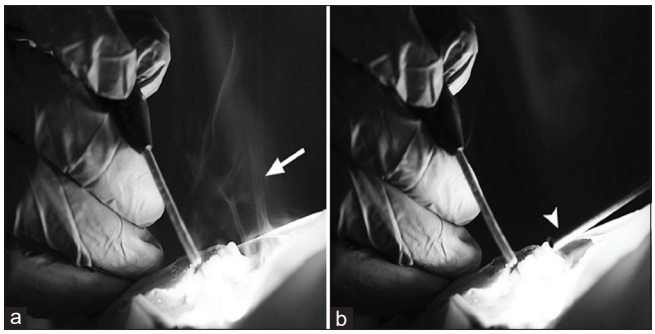

Figure 5: (a) Escaping smoke (arrow) from monopolar cautery without suction. (b) No visible escape with suction (arrowhead)

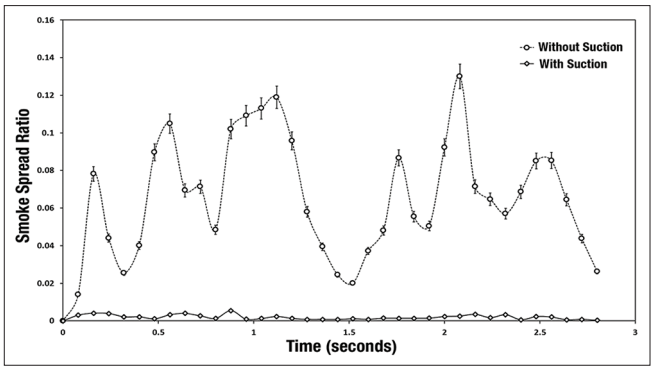

Figure 6: Time history of smoke spread for monopolar cautery with and without suction. The circle represents smoke spread without use of suction, and the diamond represents spread of smoke with use of suction

smoke) is also categorized as an aerosol.[19] It comprises 95% air and 5% solids or liquids suspended in the air.

In respiratory infections, infective particles range in size from 0.5 μm to 500 μm.[20] The larger particles, or droplets, tend to settle to the ground. Smaller airborne particles evaporate faster, remain suspended in the air and will be transmitted for greater distances. The size limit between the airborne and droplet particles has been variously mentioned as 5 and 10 microns by different authorities.[8,20,21] In addition, the chance of infection depends on the number of particles generated, the type of pathogen and the load of pathogen.[20]

Use of suction during induction of anesthesia has been noted as one of the maneuvers which generate aerosol.[8] Under the experimental conditions, the use of a gentle suction on a wet surgical field while using a scalpel did not generate aerosol. However, in the operating room conditions, a blood vessel may spurt forcefully; the greater speed would cause a layer of fluid to get detached and form droplets. Hence, we are unable to conclude that use of scalpel and suction causes no aerosolization.

Jewett *et al*.[22] studied the particle size generated by various surgical techniques. The oscillating bone saw, high-speed drill, electrocautery in both cutting and coagulation mode- all generated aerosols with particle sizes in the respirable range.[22]

Surgical smoke can be generated by a variety of electro-surgical devices.[19] The amount of smoke and the size of the particles depend on the type of tissue as well the energy source of the surgical device.[19,23] Hepatitis B virus, human immunodeficiency virus (HIV) and human papillomavirus (HPV) have been detected in surgical smoke.[23] Occupational exposure to surgical smoke has been associated with HPV infections.[23,24] There is insufficient evidence of spread of SARS by surgical smoke.[24] However, in order to reduce potential risk, the recommendations from the various guidelines mention avoidance of monopolar (cutting) cautery, and use of bipolar (coagulation) cautery with low power settings.[10,12] In the experiments, there was significant surgical smoke/aerosol generated by use of electrocautery in both cutting and coagulation modes. The smoke could be controlled by use of a suction device placed close to the electrosurgical probe.

Surgical smoke can be managed by the operating room ventilation systems, personal masks, or by local use of surgical smoke evacuators. Almost 80% of the particles in surgical smoke have diameters less than 5 microns, and can pass through a standard surgical mask.[23] The high-efficiency particle filters (HEPA) filters are effective, and the N95 respirator mask may filter out 95% of 0.3 micron particles depending on the make.[25] A surgical smoke evacuator, with a minimum suction capacity of 0.012 m^3/s and a triple filter, can further control the spread of the smoke.[24,26]

Use of a mechanized surgical drill, and oscillating saw have been proven to generate aerosols.[22] In a simulation of a mastoidectomy with a high-speed drill, the particle spread was 360°, with the highest concentration towards the surgeon.[27] Some guidelines advised the use of drill without irrigation.[9] In our experiment with the surgical drill, copious droplets were generated with or without irrigation. The majority of the droplets generated were in the range of 50 μm to 550 μm, which can be blocked by N95 respirator masks and personal protective equipment.[25]

The propensity of droplet formation increases with a thicker layer of fluid, and a faster motion of the instrument over the fluid.[28,29] We concluded that lesser volume of irrigation and the use of a smaller burr at a lower speed will reduce the generation of droplets. The spread diameter of the droplets encompassed the area occupied by personnel in the operating room, and all such people need to adopt precautions.

The study pertained to the physical spread of aerosol and droplets during surgery. The transmission of virus also depends on the load of viable pathogen in the aerosol.[16] Air-borne mode has also been implicated in the transmission of the virus.[3] Keeping these factors in mind, we would urge all surgeons to follow universal precautions of asepsis, use personal protection equipment and assess the urgency of the surgery.

The authors accept that an *ex vivo* study has its own limitations. However, acquisition of images for these experiments needed both accuracy and precision, as well as multiple sets of readings. In addition, use of the specified scientific equipment requires technical finesse and a prolonged duration: the total time taken for the experiments was about 10 hours. Repeated procedures in a single human subject (patient) would be unethical; readings taken in different patients would not reproduce the exact conditions of the physical surroundings. Our existing knowledge of aerosol generation in surgical settings is derived from laboratory studies.[24,30,31] We opted for our experimental set-up with these factors in mind. We chose the animal tissue for the

experiments while attempting to simulate a clinical setting as far as possible.

Conclusion

In conclusion, the use of electrosurgical devices generated surgical smoke in both cutting and coagulation modes. The spread of this smoke can be controlled significantly with use of suction apparatus. The use of a mechanized drill generated droplets with a spread extending to the surgeon and other personnel in the operating theater. A slower rotation and a smaller burr can reduce the number of droplets generated, and the N95 mask can protect the airway from the majority of the particles.

Ophthalmic practice in India has been severely affected by the COVID-19 pandemic. A survey found that nearly 60% of Indian ophthalmologists felt that they were at a higher risk than other medical specialities; they were hesitant about elective surgeries and the guidelines to follow.[32] The quantification of the aerosol generation will help surgeons take practical decisions in their surgical techniques in the pandemic era.

Financial support and sponsorship

Nil.

Conflicts of interest

There are no conflicts of interest.

References

1. Reported cases or deaths by Country Territory or conveyance. Available from: https://www.worldometers.info/coronavirus/. [Last accessed on 2020 Oct 17].
2. The Lancet. COVID-19: Protecting health-care workers. Lancet 2020;395:922.
3. Transmission of SARS-CoV-2: Implications for infection prevention precautions. Available from: https://www.who.int/publications/i/item/modes-of-transmission-of-virus-causing-covid-19-implications-for-ipc-precaution-recommendations. [Last accessed on 2020 Jul 27].
4. Wang Y, Wang Y, Chen Y, Qin Q. Unique epidemiological and clinical features of the emerging 2019 novel coronavirus pneumonia (COVID-19) implicate special control measures. J Med Virol 2020;92:568-76.
5. Kumar K, Prakash AA, Gangasagara SB, Rathod SBL, Ravi K, Rangaiah A, *et al*. Presence of viral RNA of SARS-CoV-2 in conjunctival swab specimens of COVID-19 patients. Indian J Ophthalmol 2020;68:1015-7.
6. Seah IYJ, Anderson DE, Kang AEZ, Wang L, Rao P, Young BE, *et al*. Assessing viral shedding and infectivity of tears in coronavirus disease 2019 (COVID-19) patients. Ophthalmology 2020;127:977-9.
7. Sungnak W, Huang N, Bécavin C, Berg M, Queen R, Litvinukova M, *et al*. SARS-CoV-2 entry factors are highly expressed in nasal epithelial cells together with innate immune genes. Nat Med 2020;26:681-7.
8. Infection prevention and control of epidemic - and pandemic-prone acute respiratory diseases in health care. Available from: https://apps.who.int/iris/bitstream/handle/10665/69707/WHO_CDS_EPR_2007.6_eng.pdf; jsessionid=F2FDB0C62789045E459DD4DE609F4574?sequence=1. [Last accessed on 2020 Jun 15].
9. AO CMF International Task Force Recommendations on Best Practices for Maxillofacial Procedures during COVID-19 Pandemic. Available from: https://www.aofoundation.org/-/media/project/aocmf/aof/documents/ao-cmf-covid19-guidelines.pdf. [Last accessed on 2020 Jun 08].
10. Guidelines for the oculoplastic and ophthalmic trauma surgeon during the covid-19 era. Available from: https://apsoprs.org/news/guidelines-for-the-oculoplastic-and-ophthalmic-trauma-surgeon-during-the-covid-19-era. [Last accessed on 2020 Jun 12].
11. Sengupta S, Honavar SG, Sachdev MS, Sharma N, Kumar A, Ram J, *et al*. All India Ophthalmological Society - Indian Journal of Ophthalmology consensus statement on preferred practices during the COVID-19 pandemic. Indian J Ophthalmol 2020;68:711-24.
12. Ali MJ, Hegde R, Nair AG, Bajaj MS, Betharia SM, Bhattacharjee K, *et al*. All India Ophthalmological Society - Oculoplastics Association of India consensus statement on preferred practices in oculoplasty and lacrimal surgery during the COVID-19 pandemic. Indian J Ophthalmol 2020;68:974-80.
13. Otsu N. A threshold selection method from gray-level histograms. Automatica 1975;11:23-7.
14. Sbalzarini IF, Koumoutsakos P. Feature point tracking and trajectory analysis for video imaging in cell biology. J Struct Biol 2005;151:182-95.
15. Shetty N, Kaweri L, Khamar P, Balakrishnan N, Rasheed A, Kabi P, *et al*. Propensity and quantification of aerosol and droplet creation during phacoemulsification with high-speed shadowgraphy amidst COVID-19 pandemic. J Cataract Refract Surg 2020;46:1297-301.
16. Khamar P, Shetty R, Balakrishnan N, Kabi P, Roy D, Basu S, *et al*. Aerosol and droplet creation during oscillatory motion of the microkeratome amidst COVID-19 and other infectious diseases. J Cataract Refract Surg 2020. doi: 10.1097/j.jcrs. 0000000000000326. Epub ahead of print.
17. Rothan HA, Byrareddy SN. The epidemiology and pathogenesis of coronavirus disease (COVID-19) outbreak. J Autoimmun 2020;109:102433.
18. Tang JW, Li Y, Eames I, Chan PK, Ridgway GL. Factors involved in the aerosol transmission of infection and control of ventilation in healthcare premises. J Hosp Infect 2006;64:100-14.
19. Mintz Y, Arezzo A, Boni L, Baldari L, Cassinotti E, Brodie R, *et al*. The risk of COVID-19 transmission by laparoscopic smoke may be lower than for laparotomy: A narrative review. Surg Endosc 2020;34:3298-305.
20. Gralton J, Tovey E, McLaws ML, Rawlinson WD. The role of particle size in aerosolised pathogen transmission: A review. J Infect 2011;62:1-13.
21. Austin E, Brock J, Wissler E. A model for deposition of stable and unstable aerosols in the human respiratory tract. Am Ind Hyg Assoc J 1979;40:1055-66.
22. Jewett DL, Heinsohn P, Bennett C, Rosen A, Neuilly C. Blood-containing aerosols generated by surgical techniques: A possible infectious hazard. Am Ind Hyg Assoc J 1992;53:228-31.
23. Vourtzoumis P, Alkhamesi N, Elnahas A, Hawel JE, Schlachta C. Operating during COVID-19: Is there a risk of viral transmission from surgical smoke during surgery? Can J Surg 2020;63:E299-301.
24. Mowbray NG, Ansell J, Horwood J, Cornish J, Rizkallah P, Parker A, *et al*. Safe management of surgical smoke in the age of COVID-19. Br J Surg 2020;107:1406-13.
25. Liu Y, Song Y, Hu X, Yan L, Zhu X. Awareness of surgical smoke hazards and enhancement of surgical smoke prevention among the gynecologists. J Cancer 2019;10:2788-99.
26. Fencl JL. Guideline implementation: Surgical smoke safety. AORN J 2017;105:488–97.
27. Chen JX, Workman AD, Chari DA, Jung DH, Kozin E, Lee DJ, *et al*. Demonstration and mitigation of aerosol and particle dispersion during mastoidectomy relevant to the COVID-19 era. Otol Neurotol 2020;41:1230-9.
28. Pandey K, Basu S. How boiling happens in nanofuel droplets. Phys Fluids 2018;30:107103.
29. Pathak B, Basu S. Phenomenology of break-up modes in contact free externally heated nanoparticle laden fluid droplets. Phys Fluids 2016;28:123302.
30. Heinsohn P, Jewett DL, Balzer L, Bennett CH, Seipel P, Rosen A. Aerosols created by some surgical power tools: Particle size distribution and qualitative hemoglobin content. Appl Occup Environ Hyg 1991;6:773-6.
31. Johnson GK, Robinson WS. Human immunodeficiency virus-1 (HIV-1) in the vapors of surgical power instruments. Med Virol 1991;33:47-50.
32. Nair AG, Gandhi RA, Natarajan S. Effect of COVID-19 related lockdown on ophthalmic practice and patient care in India: Results of a survey. Indian J Ophthalmol 2020;68:725-30.